Electronic Supplementary Material (ESI) for Journal of Materials Chemistry C.

Supporting Information

Photo-responsive Diels–Alder Based Azobenzene-Functionalized Main-Chain Liquid Crystal Networks

Minwook Park, Jesus Guillen Campos, Friedrich Stricker, Javier Read de Alaniz*

Department of Chemistry and Biochemistry, University of California at Santa Barbara, Santa Barbara, California 93106, United States

javier@chem.ucsb.edu

Dryad data submission doi: doi:10.5061/dryad.jsxksn0jv

Table of Contents

1. General Experimental

1.1 Materials

All chemicals and solvents were obtained from Fisher Scientific, Sigma Aldrich, or TCI Europe and were used as is without further purification. Anhydrous solvents were dispensed from a solvent purification system immediately before use or sourced from Sigma Aldrich. For thin-layer chromatography (TLC) was conducted with E. Merck silica gel 60 F254 pre-coated plates (0.25 μm) and visualized by exposure to UV light (254 nm) or stained with $KMnO_4$ and *p*-anisaldehyde. Flash column chromatography was perfomed using normal phase silica gel (60 Å, 40 to 62 μm, Geduran) with hexanes, ethyl acetate (EtOAc), DCM and/or MeOH as eluents.

1.2 Instruments and methods

^1H and ^{13}C spectra were recorded on Bruker and Varian instruments (100, 125, 500 and 600 MHz) and reported relative to $CDCl_3$ (δ = 7.26 ppm for ^1H and 77.00 ppm for ^{13}C). Data for ^1H NMR spectra are reported as follows: chemical shift (δ ppm), multiplicity, coupling constant (Hz) and integration. Data for ^{13}C NMR spectra are reported in terms of chemical shift (δ ppm). Differential Scanning Calorimetry (DSC) measurements were performed on a TA Instruments Q2000 DSC with a sensitivity of < 0.2 μW and a baseline drift < 10 μW. The DSC experiments involved a temperature ramp from 0 °C to 140 °C, with a rate of 5 or 10 °C min^{-1}. For 1-dimensional wide-angle X-ray diffraction (1D WAXD), a powder diffractometer (Cu Kα radiation, 4 kW; Malvern Panalytical) was utilized. Additionally, 2D WAXD experiments were conducted using a diffractometer constructed by UCSB MRL X-ray facility, employing an X-ray source from XENOCS Genix 50W w-ray microsource with a wavelength of 1.54 Å. The photoinduced optical absorption kinetics were investigated using a degenerative pump-probe setup. The optical beam was generated using a high-power white light-emitting diode (LED) source from Thorlabs (model MWWHF2). The LED beam was coupled into a multimode optical fiber, which was then connected to an output collimator. The intensity of the LED beam was regulated either manually or through a digital-to-analog converter (National Instruments USB-6009) controlled by LabVIEW software. The AzoLCN cantilever motion during photo-responsive deformation was captured using a Canon EOS Rebel T5i camera equipped with a 100 mm f/2.8 macro lens. The camera had a magnification of 1x and operated at a frame rate of 30 Hz. The tip deflection during each illumination cycle was measured by tracking the position of the tip of the cantilever's end in every frame using Tracker software (Open Source Physics Project). To record the temperature of the AzoLCNs under illumination, an infrared camera (FLIR® E60) was employed. The built-in spot meter feature of the camera was utilized to select the center of the illuminated specimen and measure the temperature of that specific region in each frame. The mechanical properties of the AzoLCN films were analyzed using a Dynamic Mechanical Analyzer (DMA) (TA Instruments DMA 850) with N_2 gas cooling. The Samples were subjected to tension tests with 0.1, 1, 10 Hz oscillation frequency and 1 mN force.

2. Synthesis

2.1 Synthetic procedures

(*E*)-bis(furan-2-ylmethyl) 7,7'-((diazene-1,2-diylbis(4,1-phenylene))bis(oxy))diheptanoate (AzoFu).

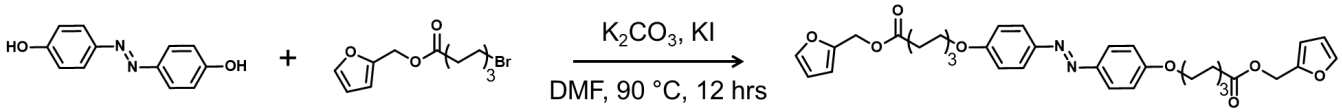

Azo diol (214.07 g/mol) | **Furan-Br** (288.04 g/mol) | **AzoFu** (630.29 g/mol)

To a round bottom flask, potassium carbonate (K_2CO_3) (2.8 g, 20.25 mmol, 4.4 eq.), potassium iodide (KI) (catalytic amount 10 mg), (*E*)-4,4'-(diazene-1,2-diyl)diphenol (Azo diol) (1 g, 4.7 mmol, 1.0 eq.) and furan-2-ylmethyl 7-bromoheptanoate (Furan-Br) (2.96 g, 10.27 mmol, 2.2 eq.) were added to 30 mL anhydrous dimethylformamide (DMF) and stirred for 12 h at 90 °C. After dilution with water (150 mL), the mixture was extracted with ethyl acetate (3 x 30 mL). The combined organic layer was dried over anhydrous magnesium sulfate ($MgSO_4$) and evaporated under reduced pressure. The residue was purified by column chromatography with silica gel using the eluent (ethyl acetate/hexane = 3:7) to yield Compound **AzoFu** as a white powder (yield 80%) after drying under high vacuum.

AzoFu: ^{1}H NMR (400 MHz, $CDCl_3$) δ: 7.85 (d, 4H), 7.41 (d, 2H), 6.97 (d, 4H), 6.40-6.35 (m, 4H), 5.07 (s, 4H), 4.01 (t, 4H), 2.36 (t, 4H), 1.80 (m, 4H), 1.68 (m, 4H), 1.49 (m, 4H), 1.39 (m, 4H). ^{13}C NMR (125 MHz, $CDCl_3$) δ: 173.20, 161.04, 149.58, 147.00, 143.25, 124.32, 114.65, 110.57, 77.34, 77.03, 76.71, 67.93, 57.96, 34.03, 28.87, 25.59, 24.62. IR (ATR) 3070, 2936, 2855, 1728, 1600, 1578, 1500, 1447, 1380, 1316, 1353, 1147, 1067, 1016, 979, 953, 912, 850, 738, 600, 573 cm^{-1}.

2.2 ^{1}H and ^{13}C NMR spectra

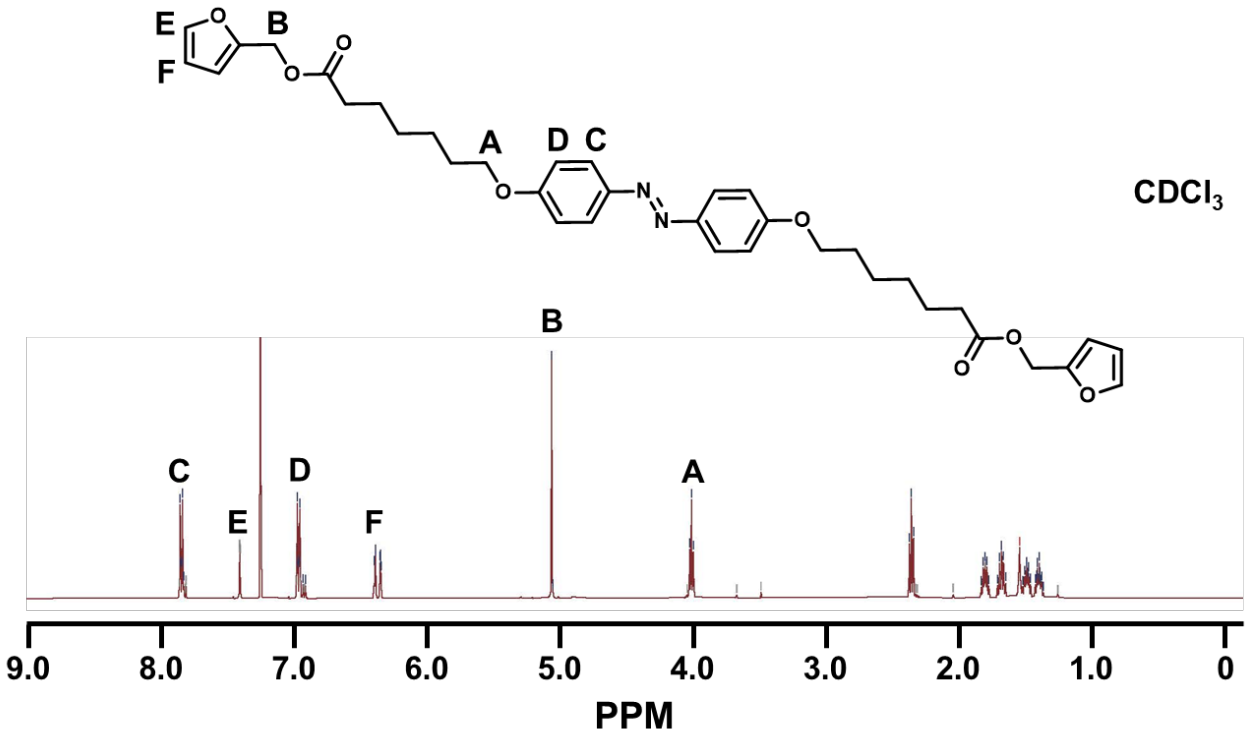

Figure S1. ^{1}H NMR spectrum of mesogenic Azofuran (**AzoFu**).

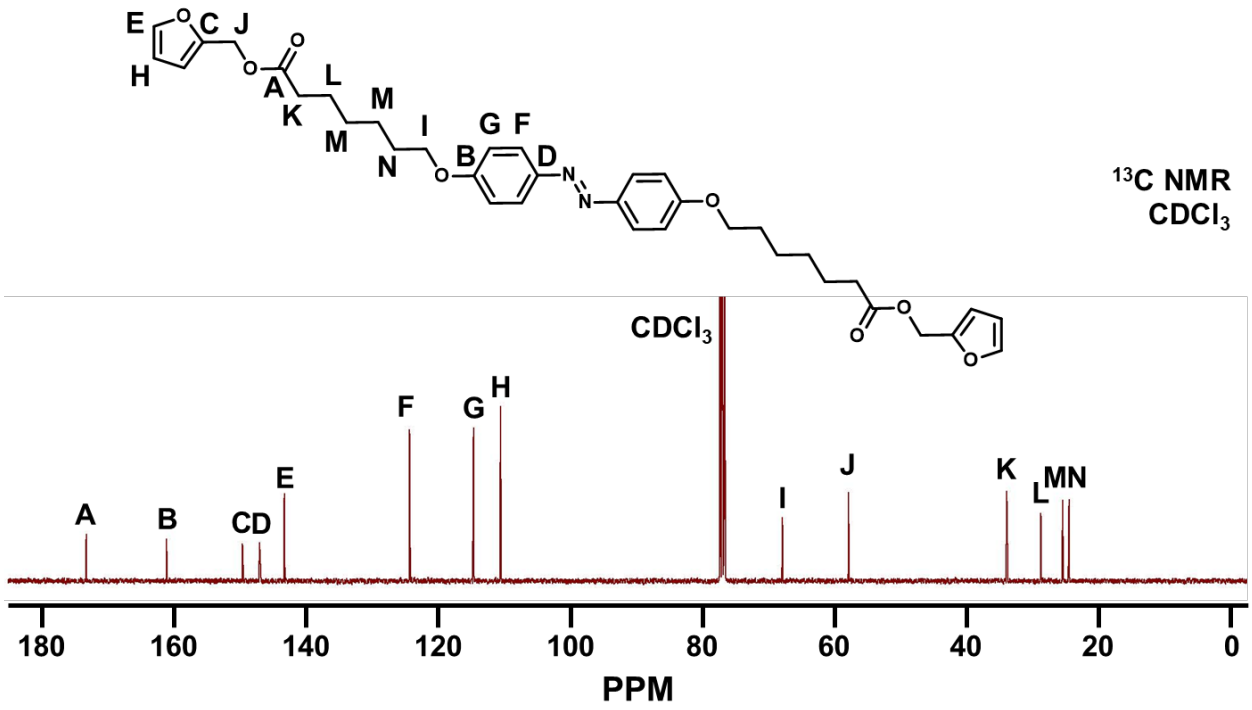

Figure S2. ^{13}C NMR spectrum of mesogenic Azofuran (**AzoFu**).

3. Thermodynamic properties (DSC) and powder X-ray diffractions (WAXD)

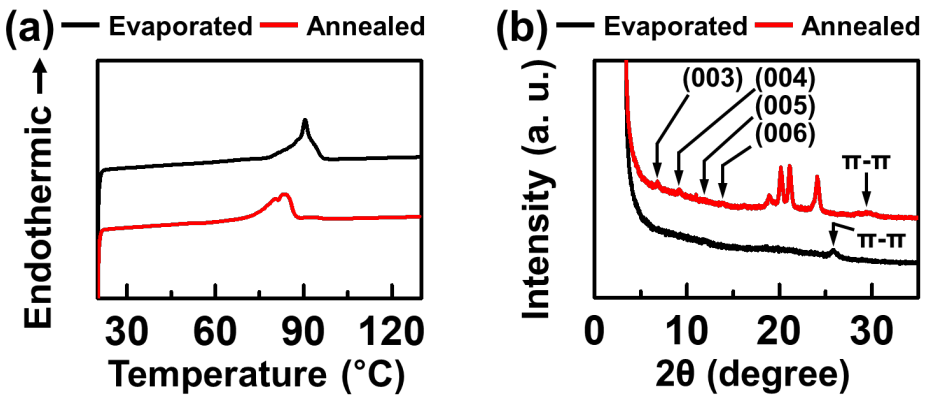

Figure S3. (a) DSC heating diagrams taken at 5 °C min^{-1} and (b) 1D powder WAXD patterns for AzoFu molecule in solvent-evaporated and annealed state.

4. Film fabrication and optical property for poly- and mono-domain AzoLCNs

The procedure of film fabrication: Clean glasses were washed and sonicated with hexane, acetone, methanol each three times. Sub-micro polyvinyl alcohol (PVA) layer was obtained via spin coating (2000 rpm for 50 s) and followed baking stage (100 °C for 1 h). For polydomain AzoLCN, these two PVA-coated glasses were just sandwiched using a cell gap tape (10 μm). For monodomain AzoLCN, before making a cell additionally rubbing step was added to rub the PVA layer by mechanical force using fine velvet cloth. A mixture was prepared by simply mixing and stirring with a minimal amount of dichloromethane for 10 min. The cell was placed on a hot plate set with each temperature (50 °C, 78 °C, and 95 °C), respectively. The mixture was dropped on the cell and dried at 50 °C to eliminate solvent for 10 min. Melted mixture was readily injected into the cell by capillary effect. The polymerization proceeded for 7 days.

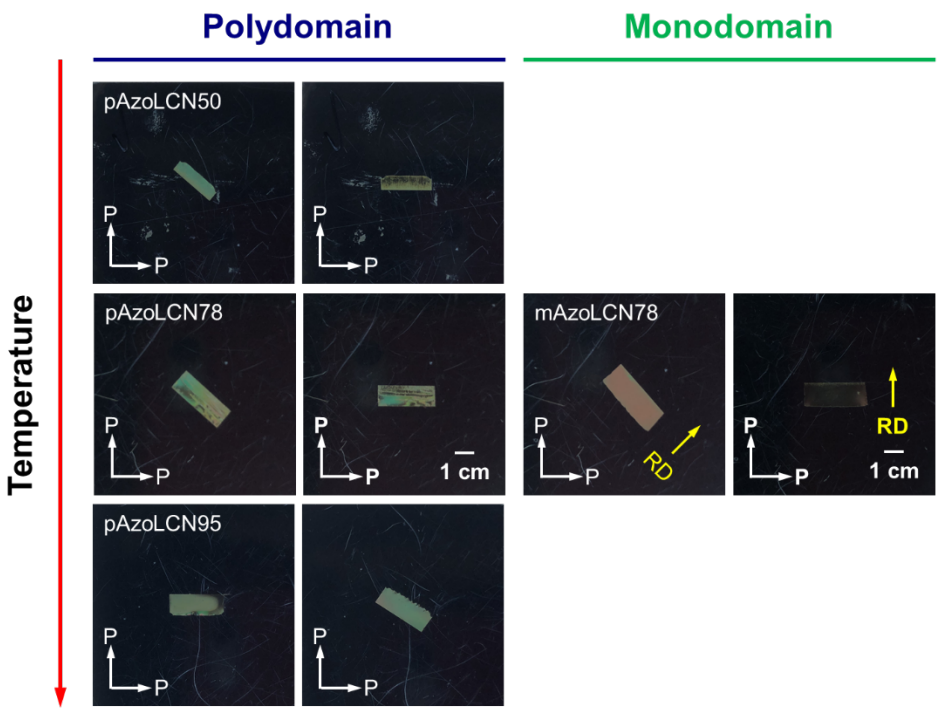

Figure S4. Images of AzoLCN films prepared at different temperatures (50 °C, 78 °C, and 95 °C) with or without help of planar alignment. These pictures were taken under crossed polarizers. P: polarizer direction, RD: rubbing direction.

5. Photo-responsive deformation of poly- and mono-domain AzoLCNs

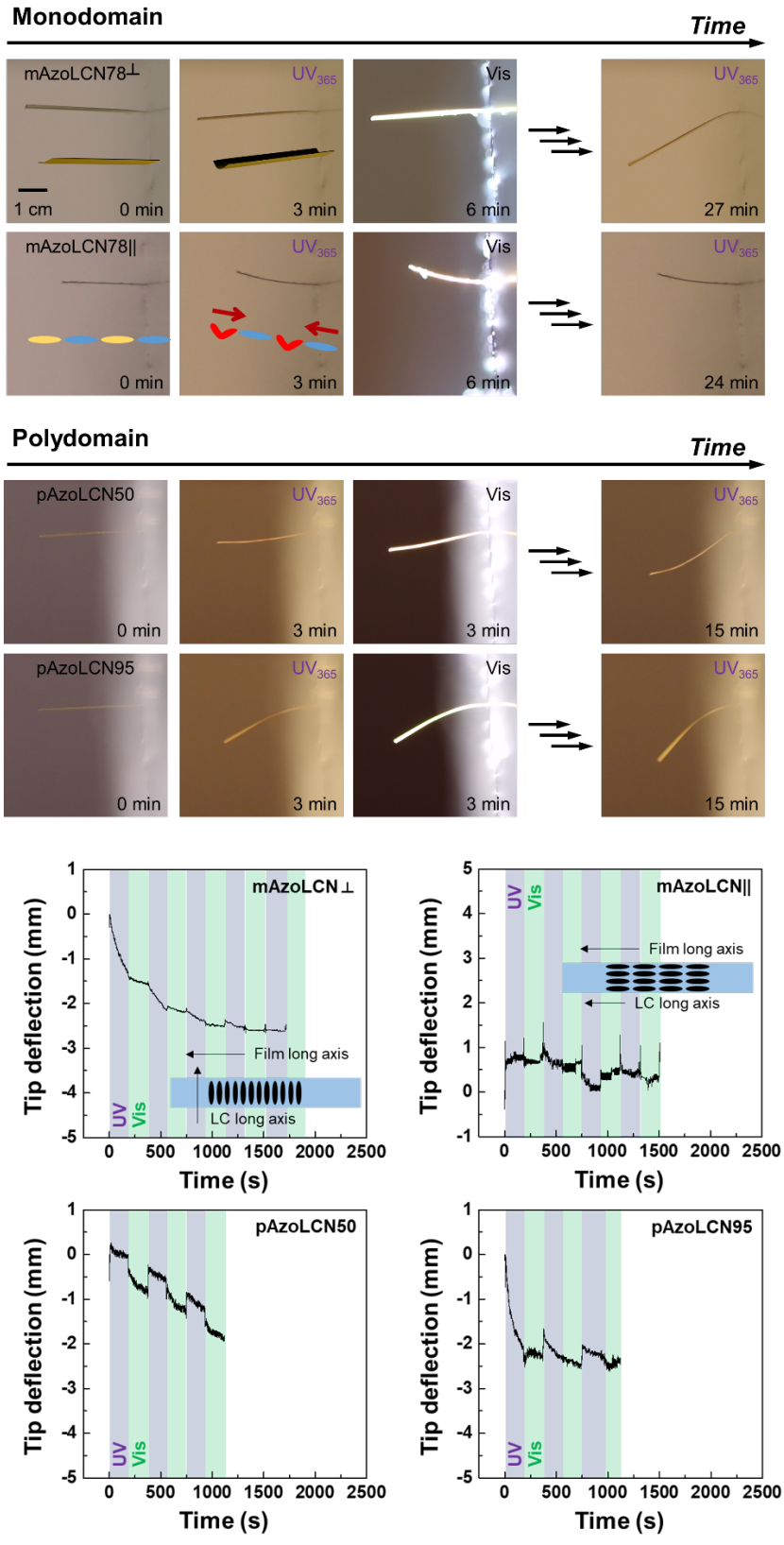

Figure S5. The images and tip deflection tracking for photo-responsive deformation behavior of pAzoLCNs and mAzoLCNs under alternative UV or visible light irradiation each for 3 min. The schemes in the graph of the tip deflection represent a top view.

6. Gravity effect on photo-responsive deformation

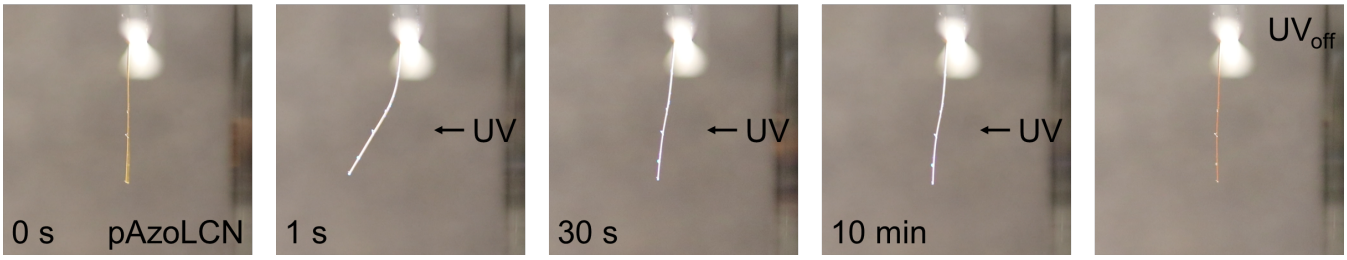

Figure S6. The images for photo-responsive deformation behavior of pAzoLCN under continuous UV light irradiation for 10 min.

7. Photo-responsive deformation dominated by molecular orientation and photochemical effect

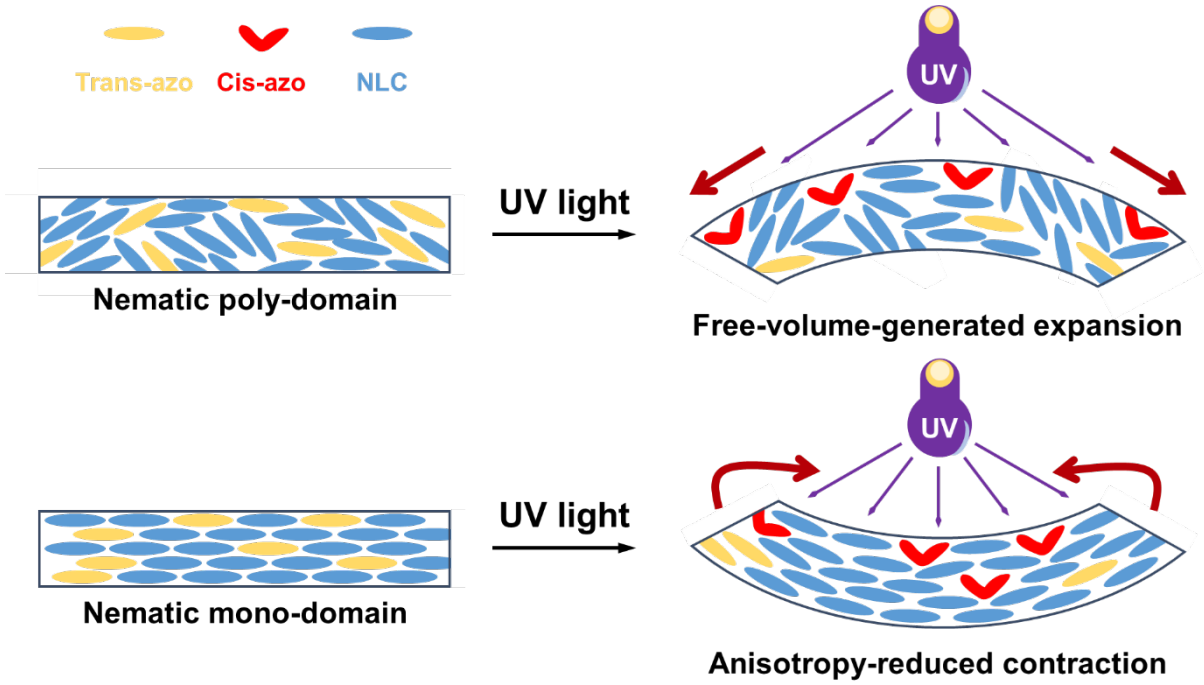

Figure S7. Schematic illustration of deforming directions of photo-responsive AzoLCNs.

8. Temperature variation tracking of LCN and AzoLCN under UV light irradiation

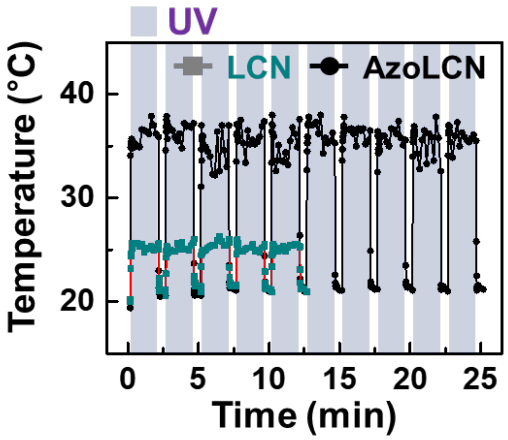

Figure S8. Temperature variation tracking of LCN and AzoLCN under alternative UV light on and off.

9. Thermodynamic property (DSC) variation depending on AzoLCN conditions

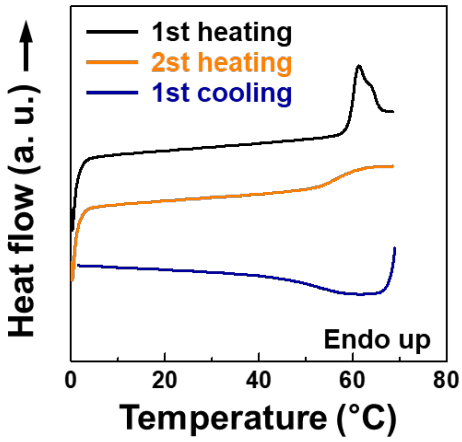

Figure S9. A set of DSC heating and subsequent cooling diagrams (5 °C min^{-1}) of AzoLCN. Temperature range during heating/cooling process is in 0 °C to 70 °C, which is slightly higher than T_g.

10. 1D WAXD of LCN under UV light on and off

To further understand the impact of photothermal and photo-chemical effects on molecular packing structure, we monitored the XRD pattern over time before and after UV light irradiation. As shown at Figure S10, a nematic structure with an average lateral packing *d*-spacing of 0.45 nm was maintained without any noticeable variation after UV light irradiation. The lack of change in quasi-long-range order indicates that light irradiation does not have a significant impact on the global molecular packing structure in the AzoLCN upon irradiation.

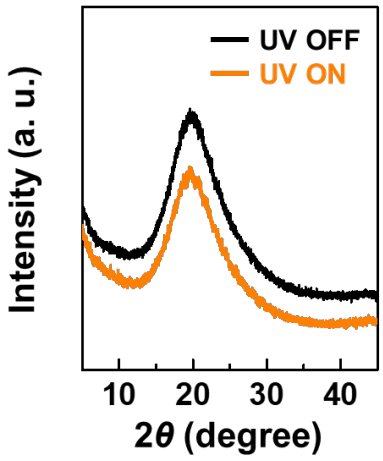

Figure S10. 1D WAXD patterns of AzoLCN before and after UV light irradiation for observation of variation of molecular packing in network.

11. Schematic illustration of programmed DMA experiment set-up

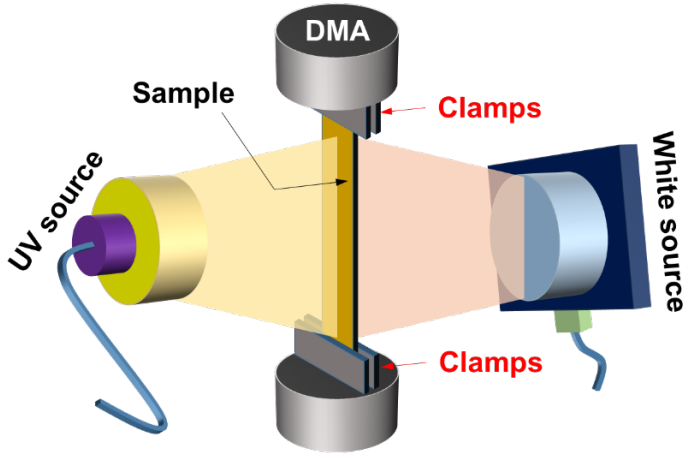

Figure S11. Schematic illustration of DMA experiments for programmed photo-responsive deformation of AzoLCN samples.

12. Mechanical property tracking of AzoLCN under a series of conditions

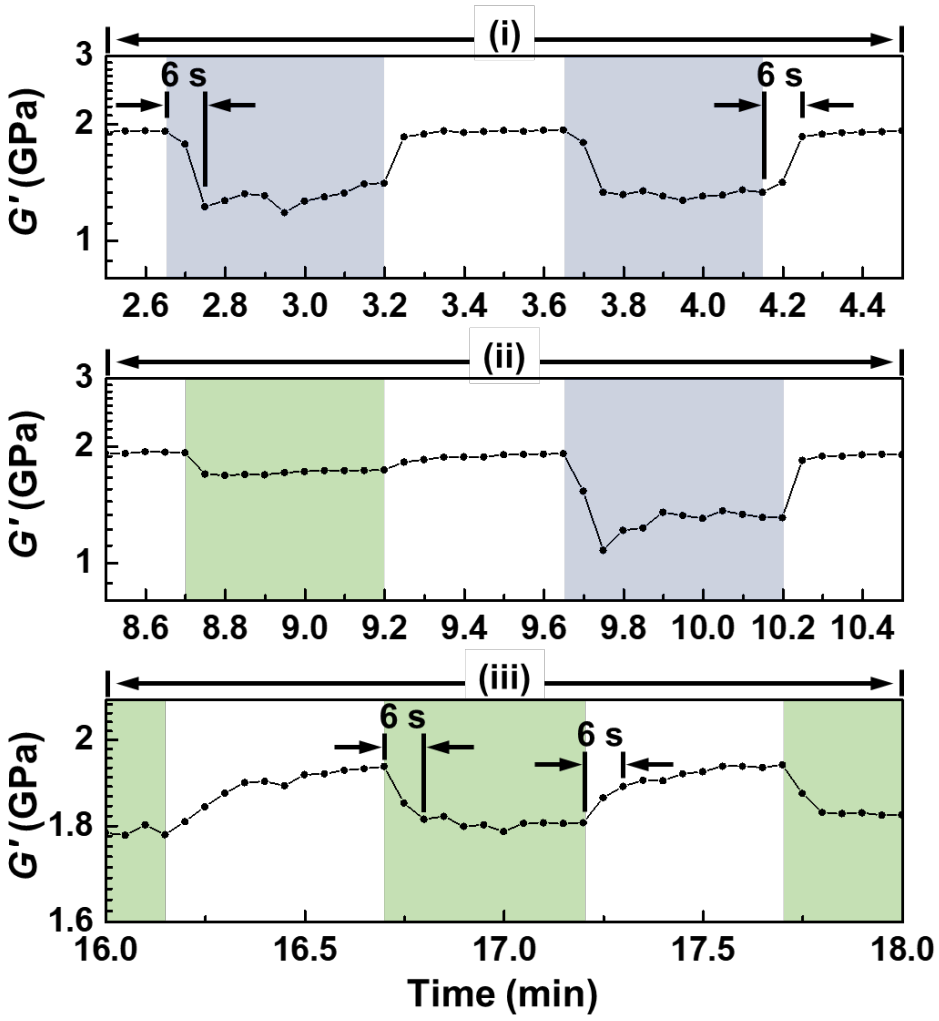

Figure S12. Storage modulus tracking of AzoLCN under (i) cycled UV light irradiation (30 seconds) and (ii) alternatively cycled UV and visible light irradiation (30 seconds each) and (iii) cycled visible light irradiation (30 seconds) at intervals of 30 seconds respectively.

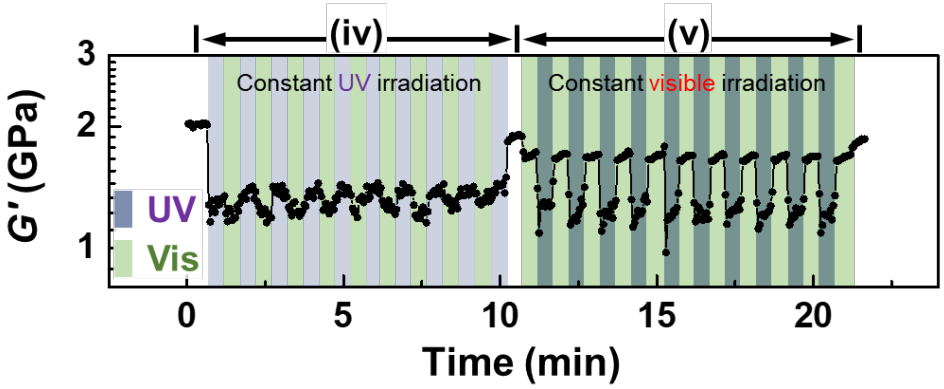

Figure S13. Storage modulus tracking of AzoLCN under (iv) constant UV light irradiation with visible light irradiation at intervals of 30 s for 9 min and (v) constant UV light irradiation with visible light irradiation at intervals of 30 s for 10 min.

13. Reversibility of mechanical property depending on amount of cross-linker and oscillation speed

The AzoLCN sample (cantilever), when fixed on one side, exhibited no recovery behavior in the UV on and off state (Figure 2). In contrast, the AzoLCN samples, where both edges were fixed for DMA experiments, exhibited the reversible mechanical properties. We hypothesized that when the network experiences high constraints on the mobility of molecular chains and is subjected to external stimuli, it would spontaneously restore to the initial state through entropy recovery upon the removal of external stimuli.[1] This constraint condition can be achieved by either increasing the cross-linking density or by fixing the LNC sample in place. To test this experimentally, a series of AzoLCN were prepared depending on the molar ratio (0%, 2%, 4%, and 10%) of the cross linker (TMal). The molecular packing structure in LC network exhibited the same nematic structure regardless of the concentration of the cross linker (Figure S13c). As shown at Figure S13a, the initial *G*' values increased (2 GPa → 2.2 GPa → 3.4 GPa) as the cross-linking density increased (2% → 4% → 10%). Furthermore, all these AzoLCN samples including the cross linker exhibited clear reversible changes in modulus. In contrast, the sample with no cross linker (0%) exhibited the lowest value (~ 1 MPa) and irreversible mechanical change regardless of UV light irradiation. It indicates that the cross-linked state, which constrain the chain mobility by immobilizing and entangling polymer chains, is essential for achieving reversible photo-responsive mechanical deformation. To investigate the correlation between oscillation speed and mechanical properties, DMA experiments at frequencies (0.1, 1, and 10 Hz) were monitored under repetitive UV light irradiation (On: 2 min, OFF: 2 min) (Figure S13b). In both cases (1 Hz and 10 Hz), the same quick response time (~4 s) was observed upon turning on or off. This indicates that it takes at least 4 cycles of stretching and releasing to achieve optimal network reorganization under influence of photothermal effect. Interestingly, under 0.1 Hz condition the reversible behavior proceeded slowly with a significantly slower response time (~120 s), spanning across ~12 cycles. These results indicate that the reversibility of the mechanical properties is highly dependent on the cross-linking density and the sample fixing condition (one vs multi-side fixing) as well as oscillation speed.

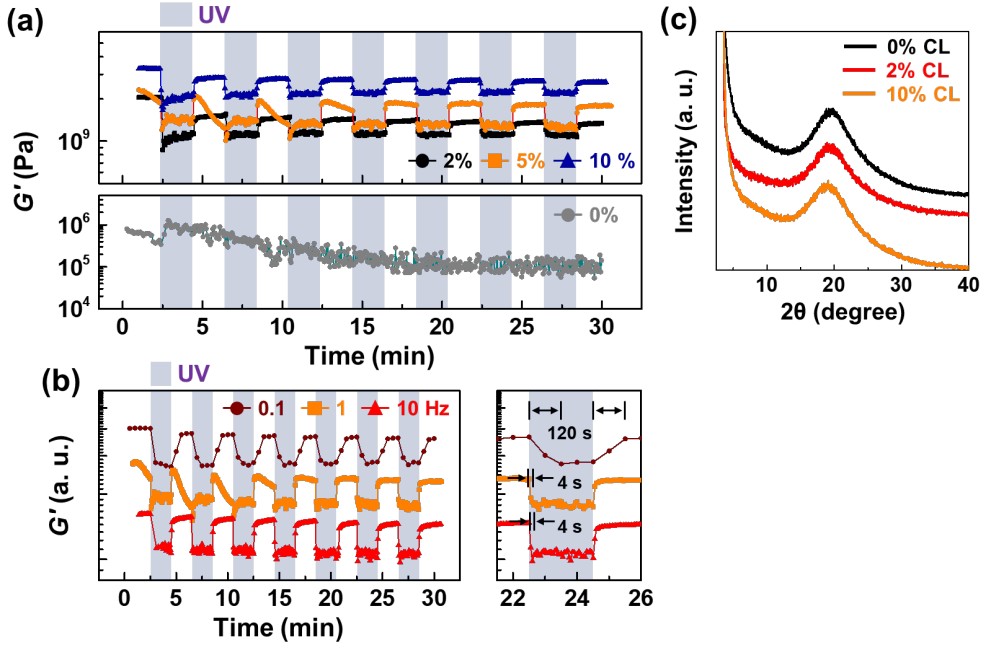

Figure S14. (a) Storage modulus tracking of different AzoLCNs with 0%, 2%, 5%, and 10% (mol%) cross-linkers and (b) Storage modulus tracking of AzoLCN under different DMA oscillation (0.1 Hz, 1 Hz, 10 Hz), under alternative UV light irradiation on and off and (c) 1D WAXD patterns of AzoLCN depending on the molar ratio of the cross-linker (0%, 2%, 10%).

Reference

[1] Xie, T. Recent advances in polymer shape memory. *Polymer* **2011**, *52*, 4985−5000.